Charge-Transfer Complexes between Tetrathiafulvalene and 1,2,5-Chalcogenadiazole Derivatives: Synthesis, Structures, Electronic and Electrical Properties

Nikolay A. Pushkarevsky,[1] Anton V. Lonchakov,[2,3] Nikolay A. Semenov,[4] Enno Lork,[5] Lev I. Buravov,[6] Lidia S. Konstantinova,[7] Georg T. Silber,[9] Neil Robertson,[9] Nina P. Gritsan,*[,2,3] Oleg A. Rakitin,*[,7] J. Derek Woollins,*[,8] Eduard B. Yagubskii,*[,6] Jens Beckmann,*[,6] Andrey V. Zibarev*[,3,4]

[1]*Institute of Inorganic Chemistry, Russian Academy of Sciences, 630090 Novosibirsk, Russia*

[2]*Institute of Chemical Kinetics and Combustion, Russian Academy of Sciences, 630090 Novosibirsk, Russia*

[3]*Department of Physics, National Research University – Novosibirsk State University, 630090 Novosibirsk, Russia*

[4]*Institute of Organic Chemistry, Russian Academy of Sciences, 630090 Novosibirsk, Russia*

[5]*Institute for Inorganic and Physical Chemistry, University of Bremen, 28334 Bremen, Germany*

[6]*Institute for Problems of Chemical Physics, Russian Academy of Sciences, 142432 Chernogolovka, Russia*

[7]*Institute of Organic Chemistry, Russian Academy of Sciences, 119991 Moscow, Russia*

[8]*School of Chemistry, University of St. Andrews, St. Andrews, Fife KY16 9ST, United Kingdom*

[9]*EaStCHEM School of Chemistry, University of Edinburgh, King's Buildings, Edinburgh EH9 3JJ, United Kingdom*

The first charge-transfer complexes of tetrathiafulvalene (**1**) with 1,2,5-chalcogenadiazole derivatives, *i.e.* with [1,2,5]thiadiazolo[3,4-c][1,2,5]thiadiazole (**2**) and 3,4-dicyano-1,2,5-telluradiazole (**3**), were prepared in the form of single crystals and structurally defined by X-ray diffraction as **1**·**2** and **1**·$\mathbf{3}_2$, respectively. Starting compound **2** was synthesized by a new efficient method from 3,4-diamino-1,2,5-oxadiazole and disulfur dichloride. The electronic structure and UV-vis spectral properties of complexes **1**·**2** and **1**·$\mathbf{3}_2$ were studied by means of DFT

calculations. The electrical properties of single crystals of the complexes were investigated revealing semiconductor properties with an activation energy of 0.34 eV for **1·2** and 0.40 eV for **1·3**$_2$. Both complexes displayed photoconductive effects with increased conductivity under white-light illumination.

1. Introduction

Tetrathiafulvalene [1] (**1**, Chart 1) is an efficient electron donor. Its 0/+1 electrochemical potential [2] is 0.33 V [3], and the HeI UPS first vertical ionization energy is ~ 6.8 eV [4]. With electron acceptors, compound **1**, as well as its various derivatives, form numerous charge-transfer (CT) complexes and radical-ion salts. Many of the compounds prepared display electrical conductivity and superconductivity as well as magnetic properties [5]. However, further progress in the field is expected, in particular, from introducing new acceptors.

Recently, derivatives of a 1,2,5-chalcogenadiazole ring system (chalcogen: S, Se, Te) featuring positive electron affinity (EA) were recognized as a new group of electron acceptors and successfully used in the preparation of new radical-anion (RA) salts revealing antiferromagnetic exchange interactions in their spin systems [6].

In this work, the interaction between compound **1** and [1,2,5]thiadiazolo[3,4-c][1,2,5]thiadiazole and 3,4-dicyano-1,2,5-telluradiazole (**2** and **3,** respectively, Chart 1) was studied and the 1 : 1 CT complex **1·2** and 1 : 2 CT complex **1·3$_2$** were prepared in the form of single crystals. Their molecular and crystal structures were obtained by single-crystal X-ray diffraction (XRD) and the electronic properties studied by DFT calculations in combination with UV-vis spectroscopy. Electrical properties of the complexes such as dark conductivity and photoconductivity were also investigated.

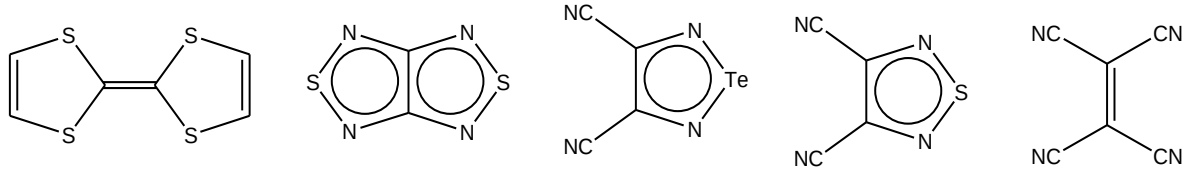

1 **2** **3** **4** **5**

Chart 1

2. Results and Discussion

2.1. Electron-acceptor properties of the heterocycles

In contrast to compound **1**, the chemistry of compounds **2** and, especially, **3** is in its infancy. Little is known besides their preparation and XRD characterization (**2** [7], **3** [8]), and the electrochemical and chemical reduction of **2** into its RA [6,7]. As for all other structurally elucidated 1,2,5-telluradiazoles, compound **3** is a coordination polymer in the solid state [8] (and references therein).

The -1/0 electrochemical potential of compound **2** is -0.59 V [7], whereas cyclic voltammetry experiments on compound **3** did not give definitive results. For S (**4**, Chart 1) and Se congeners of **3**, the -1/0 electrochemical potentials in MeCN are -1.07 and -1.03 V, respectively [9a]. From these data the potential of **3** in MeCN can be estimated as *ca.* -1.0 V. The cyclic voltammogram of **3** has complex form which depends strongly upon solvent (MeCN or DMA) and potential sweep rate, the -1/0 peak (at -0.94 V and -0.78 in MeCN and DMA, respectively) seems to be irreversible. According to the vapor-pressure osmometry data, compound **3** is monomeric in THF and DMSO solutions [8a] similar to the archetypal 1,2,5-telluradiazol [9b]. However, the experimental values of molecular weight, 236 in THF and 235 in DMSO, are slightly higher than the theoretical value 232 [8a]. Interestingly, the B97-D/def2-TZVP calculations predict existence of a dimer $\mathbf{3_2}$ in THF solution (Section 2.3). The monomer – dimer equilibrium, even shifted significantly to the left, may affect electrochemical behavior of **3**. In the light of these results the electron acceptor properties of compounds **2** and **3** were additionally studied by theoretical methods.

The first adiabatic EA of compounds **2** and **3** was calculated in the gas phase at various levels of theory. Due to the inability to perform high-level G3B3 calculations for Te containing **3**, calculations were performed with its sulfur congener **4**. For comparison, the EA of tetracyanoethylene (**5**, Chart 1) was also calculated (Table 1). As expected, the numerical results are sensitive to the level of theory whereas the zero-point energy (ZPE) correction is less significant. In recent times, DFT calculations with the B3LYP functional have been widely used for the theoretical prediction of EA [10]. Generally, it was found that the method provides somewhat higher values compared with experimental data [10,11]. For the compounds under discussion here, the values from the (U)B3LYP/6-31+G(d) calculations are close to those obtained with the high-level G3B3 technique which correctly reproduced the experimental EA of **5**. At the same time, the MP2 and PMP2 methods provided much lower values. For these reasons, the (U)B3LYP/6-31+G(d) calculations were performed for compound **3** (Table 1).

Table 1. Electron affinity (eV) of compounds calculated at various levels of theory with and

without (in parentheses) ZPE correction.

Theory / Compound	**2**	**3**[a]	**4**	**5**[b]
MP2/6-311+G(3df,2p)	1.16	1.25	0.94	2.38
PMP2/6-311+G(3df,2p)	1.48	1.67	1.33	2.93
(U)B3LYP/6-31+G(d)	2.19 (2.14)	2.16 (2.10)	1.91 (1.84)	3.51 (3.48)
(U)B3LYP/6-311+G(3df,2p)	2.07	2.05	1.86	3.50
G3B3	1.96	–	1.74	3.17

[a] Basis for Te: Def2-SVPD with diffuse basis functions and ECP. [b]Experimental value: 3.17 eV; -1/0 electrochemical potential: 0.15 V [12].

The Gibbs free energy of the electron transfer (ET) reaction between donor (D, *i.e.* **1**) and acceptor (A, *i.e.* **2** and **3**) molecules (ΔG^0) was estimated using Equation 1:

$$\Delta G^0 = E^0_{D/D^+} - E^0_{A^-/A} - \frac{e^2}{\varepsilon_s r} \quad , \qquad (1)$$

where E^0_{D/D^+} and $E^0_{A^-/A}$ are standard electrode potentials, ε_s is a solvent dielectric constant and *r* – sum of the effective radii of D and A. Assuming that $E^0_{D/D^+} \approx E^{ox}_{1/2}$ and $E^0_{A^-/A} \approx E^{red}_{1/2}$, the Gibbs free energy of the ET from **1** onto **2** in MeCN can be estimated as $\Delta G^0 \approx$ 19.3 kcal/mol. According to the calculations, ET between **1** and **2** in THF is even less favorable than in MeCN by ~ 3 kcal/mol. Most likely, the $E^{red}_{1/2}$ value for compound **3** is *ca.* -1.0 V (see above). With this value, a rough estimation of the Gibbs free energy of the ET from **1** onto **3** in MeCN gives $\Delta G^0 \approx$ 29 kcal/mol. One can conclude that formation of RA salts $[\mathbf{1}]^+[\mathbf{2}]^-$ and $[\mathbf{1}]^+[\mathbf{3}]^-$ is thermodynamically unfavorable. Nevertheless, one can expect the formation of CT complexes between **1** and **2**, and **1** and **3**.

2.2. Preparation and XRD characterization of the complexes

Starting compound **2** was synthesized by a new efficient method based on organic base-assisted condensation of 3,4-diamino-1,2,5-oxadiazole (**6**) with disulfur dichloride accompanied by exchange of the oxygen atom by the sulfur atom (Scheme 1). Compound **2** was obtained in 75 % yield. To the best of our knowledge, the only formal analogy of this exchange is the classical Yuryev reaction performed under very drastic conditions [13].

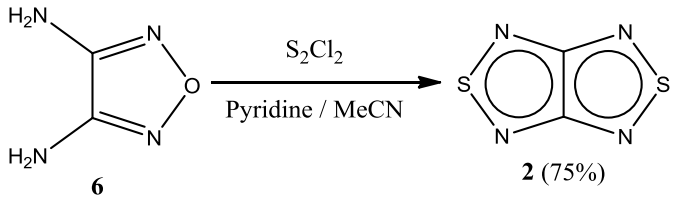

Scheme 1

The reactions between **1** and **2** and **1** and **3** were performed in THF. The reaction products were isolated from the solutions as complexes **1·2** and **1·3**$_2$, respectively, in the latter case despite the fact that the initial molar ratio of components in solution was 1 : 1. In both cases the structures of complexes were confirmed by single-crystal XRD (Figures 1 and 2).

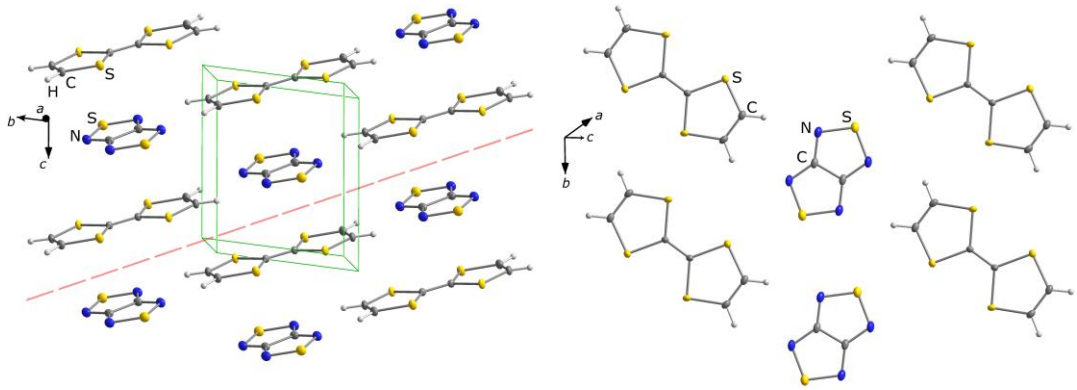

Figure 1. XRD structure of complex **1·2**. Layers containing flat D and A molecules are extended in the directions marked by the dashed line (*left*). Each layer contains the alternated rows of D and A molecules propagated along the *b* axis *(right)*. In the π-stacks, the interplanar separation is ~ 3.25 Å.

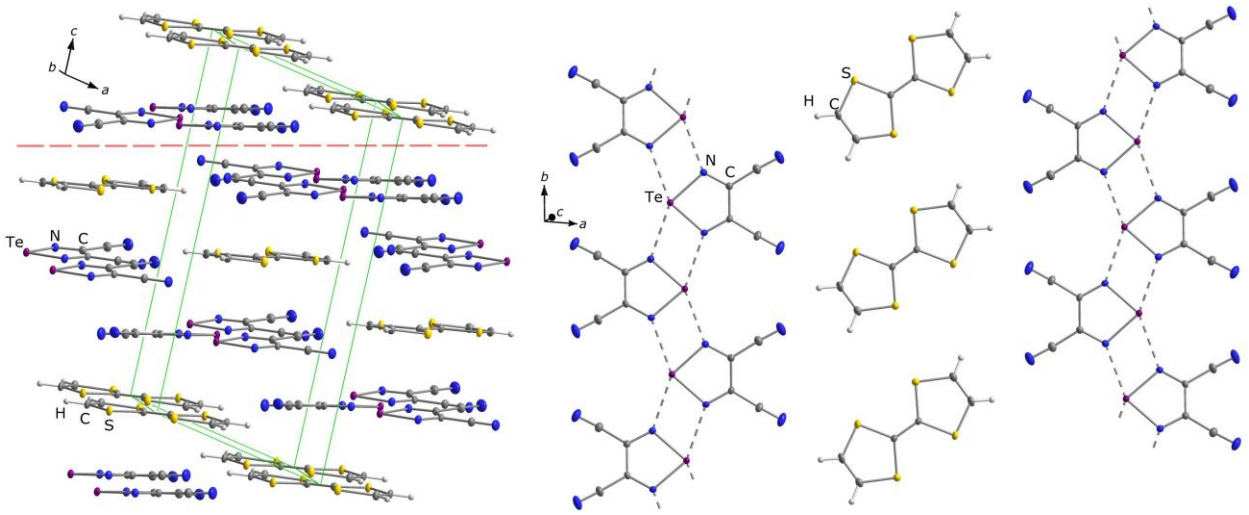

Figure 2. XRD structure of complex **1·3**$_2$. Layers containing flat D and A molecules are extended in the directions marked by the dashed line *(left)*. Each layer contains chains propagated along the *b* axis. The chains are composed of coordinatively bound molecules of **3** alternating with separate molecules of **1** *(right)*. In the π-stacks, the interplanar separation is ~ 3.26 Å.

In complexes **1·2** and **1·3**$_2$, the molecular geometries of the components (Supporting Information, Tables S1-S3) are essentially unchanged from those observed by XRD for individual **1**-**3** [7,8,14], *i.e.* they do not indicate directly the CT which, therefore, should be moderate enough (see below). Both **1·2** and **1·3**$_2$ reveal layered structures with the layers composed of flat D and A molecules (Figures 1 and 2). In both structures, the molecules of D and A in the neighboring layers form a kind of π-stacks featuring some offset leading to staircase-like motif. The layers are formed of alternating rows of **1** and **2** or **3**, respectively. In **1·2**, the maximum deviation of the molecules from the mean layer plane is 0.3 Å. The interlayer distances of 3.23 and 3.27 Å are shorter than the contact distances between D and A molecules within the layer. The packing of **1·3**$_2$ contains infinite ribbons of coordinatively bound molecules of **3**. These molecules are only slightly deflected out of the mean layer planes, the greatest deviatiation being for the CN groups (ca. 0.3 Å for the N atoms). The interlayer distances of 3.23-3.29 Å are comparable to the D…A contacts within the layer.

The polycrystalline complex **1·2** was also prepared by sublimation of ground 1 : 1 mixture of the components under static vacuum in a standard sublimation unit or sealed glass tube (Supporting Information, Figure S1). The polycrystalline complex **1·3**$_2$ was obtained by precipitation with hexane from a THF solution of the components. According to the XRD data and taking into account temperature changes of the unit cell parameters, the samples of these polycrystalline complexes have the same structures as the corresponding complexes obtained in the form of single crystals (Supporting Information, Figure S2). The observation that mixture of orange-yellow **1** and colorless **2** becomes dark-green during grinding suggests that the mechano-chemical preparation of the complex **1·2** might be possible.

2.3. Electronic structure of the complexes

To optimize structures of complexes **1·2** and **1·3**$_2$ and estimate of the thermodynamics of their formation, the B97-D functional known to be appropriate to predict the properties of weakly-bonded complexes [15] was employed. The optimized structures obtained for **1·2** and **1·3**$_2$

closely resemble those observed in the crystal (Figure 3) including the mutual orientation of, and distances between, the neighboring molecules. The compounds can be justifiably considered as CT complexes because their formation leads to transfer of 0.24e from **1** onto **2** and 0.39e from **1** onto two molecules of **3** (the CT was calculated from Mulliken charges of partner molecules, Figure 3). The optimized structure of 1 : 1 complex between **1** and **3** was not found.

To analyze bonding interactions in the complexes, a QTAIM approach [16] was applied. The first evidence of the bonding according to the approach is the existence of a bond path between two atoms and of a bond critical point (BCP) in the middle of the path.

For **1·2** the QTAIM calculations identified five BCPs related to bonding between **1** and **2**, namely, BCPs for C4…N4, C2…N3, S4…N1, S1…N2 and S2…S6 bonding. All these BCPs (Figure 3) are characterized by similar very low electron density (ρ_{BCP} = 0.5 – 1.1 × 10^{-2} a.u.) and positive values of the Laplacian ($\nabla^2\rho_{BCP}$ = 1.6 – 2.6 × 10^{-2} a.u.). The latter is typical of the closed-shell D…A interactions [16].

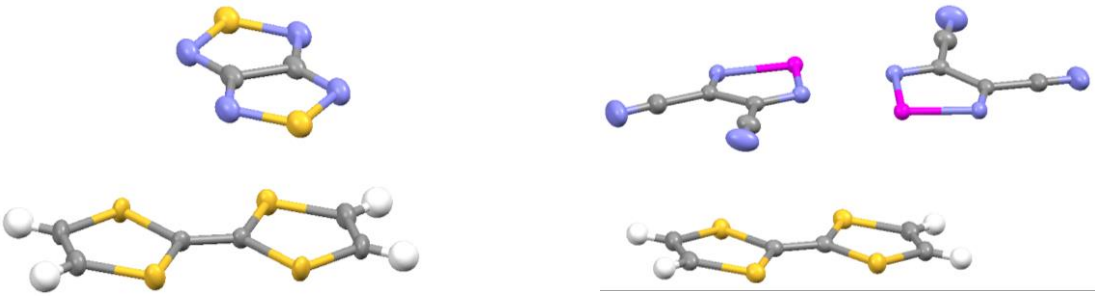

A **B**

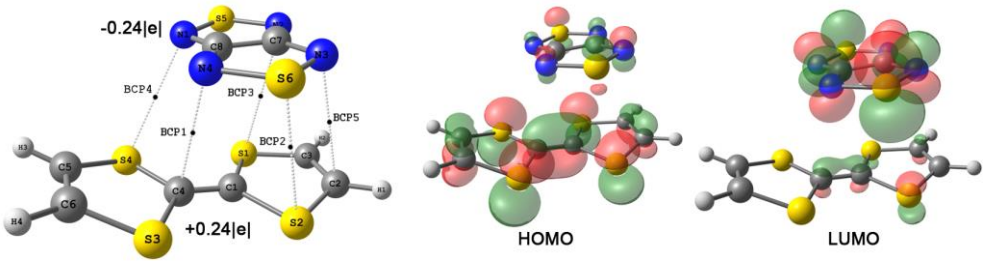

C

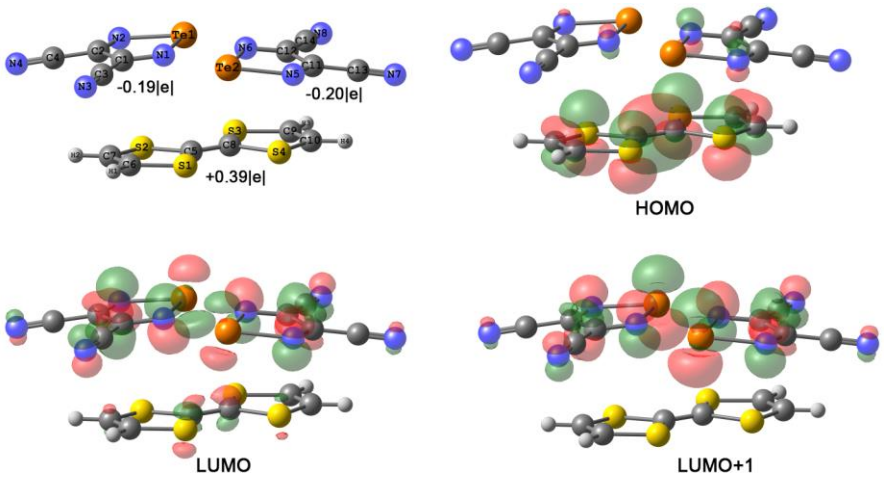

D

Figure 3. A) Orientations of the neighboring molecules in the crystal of complex **1·2**. B) Orientations of the neighboring molecules in the crystal of complex **1·3**$_2$. C) The structure of complex **1·2** optimized at the B97-D/def2-TZVP level and its frontier MOs. Selected distances (Å): S1-S5 3.922, S2-S6 3.452, S4-S5 4.679, S3-S6 4.228, N4-C4, 3.211, S1-C7 3.481, N1-S4 3.575, C2-N3, 3.468. Properties of selected BCPs (ρ_{BCP}, $\nabla^2\rho_{BCP}$ in a.u.): BCP1 (7.71×10^{-3}, 2.43×10^{-2}), BCP2 (1.08×10^{-2}, 2.62×10^{-2}), BCP3 (6.69×10^{-3}, 2.07×10^{-2}), BCP4 (5.45×10^{-3}, 1.61×10^{-2}), BCP5 (4.95×10^{-3}, 1.59×10^{-2}). D) The structure of complex **1·3**$_2$ optimized at the B97-D/def2-TZVP level with ECP on Te atoms and its frontier MOs. Selected distances (Å): Te1-Te2 3.794, Te1-N6 2.518, N1-Te2 2.606, Te1-C5 3.658, C8-N6 3.773, S1-N1 3.531, N6-S4 3.653.

According to the B97-D/def2-TZVP calculations, the enthalpy of the **1·2** formation is equal to -7.5 in THF. In turn, the Gibbs free energy is equal to 3.7 kcal/mol. Thus, the equilibrium constant for the complex formation is predicted to be 2×10^{-3} l/mol in THF, *i.e.* very low.

Formation of complex **1·3**$_2$ is thermodynamically more favorable with ΔH = -27.3 kcal/mol and ΔG = -2.8 kcal/mol in THF at the same level of theory with ECP for Te.

Thus, according to the calculations the complexes are weakly-bonded. In THF solution in the case of **1** and **2**, a new very broad absorption band with a maximum at ~ 600 nm was observed only at concentrations as high as ~ 0.02 M of both compounds (Figure 4A). In the case of **1** and **3**, the spectrum of 0.05 M 1 : 1 mixture of the reagents also revealed a new very broad absorption which manifests itself as a tail in the 500-700 nm region (Figure 4B). Figure 4

demonstrates that in the latter case the new absorption is shifted to the blue compared to that for a mixture of **1** and **2**. Figure 4C displays for comparison UV-vis spectra of **1**, **2** and **3** in MeCN which is transparent in the UV region.

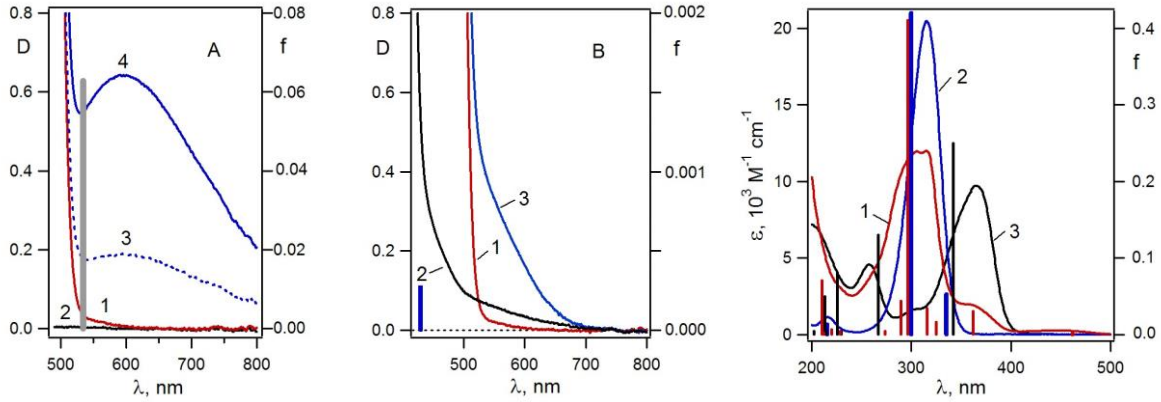

Figure 4. A) UV-vis spectra of 0.05 M solutions of **1** (1) and **2** (2), and an equimolar mixtures of **1** and·**2** with 0.025 M (3) and 0.05 M (4) concentrations in THF. Vertical bar – long-wavelength transition predicted for the CT complex **1·2** (Figure 3C) at the TD-M06HF/6-31+G(d) level. B) UV-vis spectra of compounds **1** (1), **3** (2) and an equimolar mixture of **1** and·**3** (3) with 0.05 M concentration in THF. Vertical bar – long-wavelength transition predicted at the TD-M06HF/def2-SVP level (with ECP for Te) for CT complex **1·3**$_2$ (Figure 3D). C) UV-vis spectra of **1** (1), **2** (2), and **3** (3) in MeCN solutions. Vertical bars – electronic transitions predicted for compounds **1** (red), **2** (blue) and **3** (black) at the TD-B3LYP/def2-SVPD level (for Te with ECP).

Theoretical UV-vis spectra of starting compounds **1**-**3** calculated by TD-B3LYP method agree well with experiment (Figure 4C). The absorption spectrum of complex **1·2** was calculated using M06-HF functional which is known to be appropriate for calculations of the CT states [17]. In fair agreement with experiment, calculations predict a long-wavelength transition at 530 nm (Figure 4A, vertical bar) composed mainly of the HOMO → LUMO excitation. Since these MOs have different spatial localization (Figure 3C), the excitation is accompanied by the CT from **1** onto **2**. Thus, this band can be considered as a CT band. As expected [18], the TD-B3LYP calculations underestimate significantly the energy of this CT transition (λ_{calc} = 1133 nm).

For complex **1·3**$_2$, calculations at the TD-B3LYP/def2-SVP level predict two CT bands with maxima at 776 and 959 nm. These transitions are composed of the HOMO → LUMO and

HOMO → LUMO+1 electron excitations. The HOMO is located on **1** while the LUMO and LUMO+1 are bonding and antibonding combinations, respectively, of the LUMOs of individual heterocycles **3** (Figure 3D) The TD-M06-HF/def2-SVP calculations predict a long-wavelength transition at 430 nm in better agreement with experiment (Figure 4B, vertical bar). However, this transition is composed of a complex mixture of electronic excitations.

Interestingly, the B97-D/def2-TZVP calculations predict the existence of dimers $\mathbf{3}_2$ in THF solution (Figure 5). For their formation, the ΔH is equal to -10.7 and -11.2 kcal/mol with and without BSSE correction [19], respectively. In turn, ΔG is predicted to be -0.2 and -0.6 kcal/mol, respectively. Most likely, the long-wavelength tail in the UV-vis spectrum of concentrated solution of **3** (Figure 4B, black spectrum) is due to these dimers. For **2**, formation of a dimer (Figure S3) in THF solution is expected [20,21] to be much less favorable (ΔH = -0.8 and -1.0, ΔG = 7.0 and 6.7 kcal/mol with and without BSSE correction, respectively). Most likely, thermodynamically favorable dimers $\mathbf{3}_2$ is the reason of the formation of the 1 : 2 complex $\mathbf{1}\cdot\mathbf{3}_2$ in contrast to 1 : 1 complex formed by **1** and **2**.

The QTAIM analysis of intermolecular bonding interactions in the dimer $\mathbf{3}_2$ identified two BCPs for Te1…N5 and Te2…N2 interactions (Figure 5). These BCPs (Figure 6) are characterized by low electron density (ρ_{BCP} = 0.04 a.u.) and positive values of the Laplacian ($\nabla^2\rho_{BCP}$ = 0.093 a.u.) which is typical of interactions of closed-shell species [16].

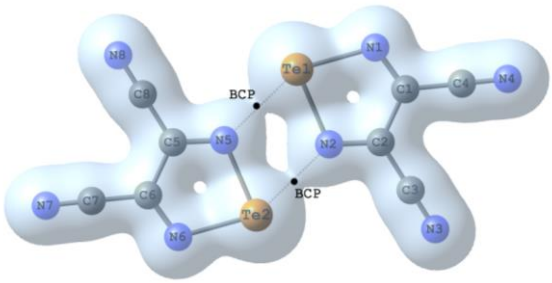

Figure 5. The structure of dimer $\mathbf{3}_2$ optimized at the B97-D/def2-TZVP level, and isosurface of the electron density (ρ = 0.035 a.u.). Selected distances (Å): Te1-N5 and N2-Te2 2.666; Te1-N2 and Te2-N5 2.027; Te1-N1 and Te2-N6 2.021.

2.4. Thermal stability and electrical properties of the complexes

According to the data of thermal analysis, upon heating in a helium atmosphere under normal pressure complex **1·2** melted at 97°C (sharp endothermic effect), and then the sample began to lose weight due to evaporation which ceased at 220°C. The thermal behavior of complex $\mathbf{1}\cdot\mathbf{3}_2$

was very different. The sample retained its weight up to 190°C, and then a sharp exothermic effect was observed with maximum at 221°C featuring 18.4 % loss of initial weight. To 300°C, 62 % of the initial weight was lost, and then the sample weight was practically constant up to 500°C.

At ambient temperature and with conventional X-band EPR technique, complexes **1·2** and **1·3**$_2$ are EPR-silent in the solid state.

The electrical properties of the complexes **1·2** and **1·3**$_2$ were studied using single crystals. Because of the low conductivity of the crystals the measurements of temperature dependence of resistance were performed in the temperature range 300-320 K (Figure 6). The resistance of the crystals at T = 300 K was ~ $2 \cdot 10^8$ Ohm.cm for complex **1·2** and 10^7 Ohm.cm for complex **1·3**$_2$. As follows from Figure 6, both complexes revealed semiconductor behavior with activation energy ~ 0.34 eV for **1·2** and 0.40 eV for **1·3**$_2$.

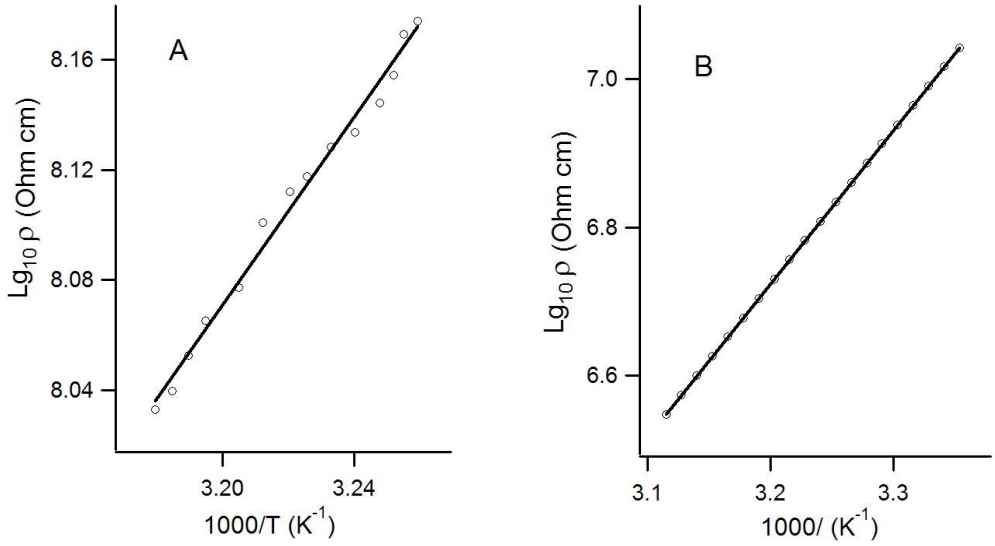

Figure 6. Temperature dependence of the resistance of single crystals of CT complexes **1·2** (A) and **1·3**$_2$ (B): circles – experiment, straight lines – the best approximations with a slope 1.70 ± 0.04 (A) and 2.08 (B).

To further investigate the electrical properties of the complexes, photoconductivity measurements were carried out using AM1.5 white light with 0.5 and 1.5 sun intensity. Photoconductivity measurements of charge-transfer salts are uncommon, probably due to the difficulty of such studies on brittle, crystalline material, although photoinduced phase transitions using laser excitation have previously attracted attention [22].

An interdigitated electrode array was used to maximize the length-to-width ratio (gain factor). Electrode gaps (channel length) of 8 and 20 μm were used. A glass substrate was chosen

over more typical Si/SiO_2 wafers to combine the benefits of direct (back) irradiation of the conductive channel with the convenience of a bottom contact setup. In particular, this was necessary as charge transfer salts cannot be easily deposited as thin films of well controlled thickness by common vapour or solution processing techniques. Instead the material was deposited onto the interdigitated electrodes using a pseudo-drop casting method [23] and, in the case of **1·2**, also by melting and recrystallizing the sample onto the substrate. Due to the non-uniformity of the polycrystalline films, comparison of the absolute values between different chips is inappropriate. The photoconductive effect, however, if expressed as the ratio of the device resistance during light and dark measurements, can be compared as it is independent of both the gain factor and the effective coverage.

$$R_{Light}/R_{Dark} = (\delta V_{Light}/\delta I_{Light}) / (\delta V_{Dark}/\delta I_{Dark})$$

The I-V characteristics for devices using gold or platinum electrodes (Figure 7a) with compound **1·3**$_2$ showed a 1.8 and 1.4 fold increase in resistivity for dark over 1.5 sun measurements, respectively. Interestingly, in the dark the platinum chip deviated slightly from ideal Ohmic behaviour. This was attributed to the charge injection barrier at the metal/semiconductor interface, which grows both in size, due to the increased mismatch between valence orbitals and metal work function (Au: 5.1eV, Pt: 6.1eV), and in relevance, as the voltage drop across the interface increases with dropping channel length.

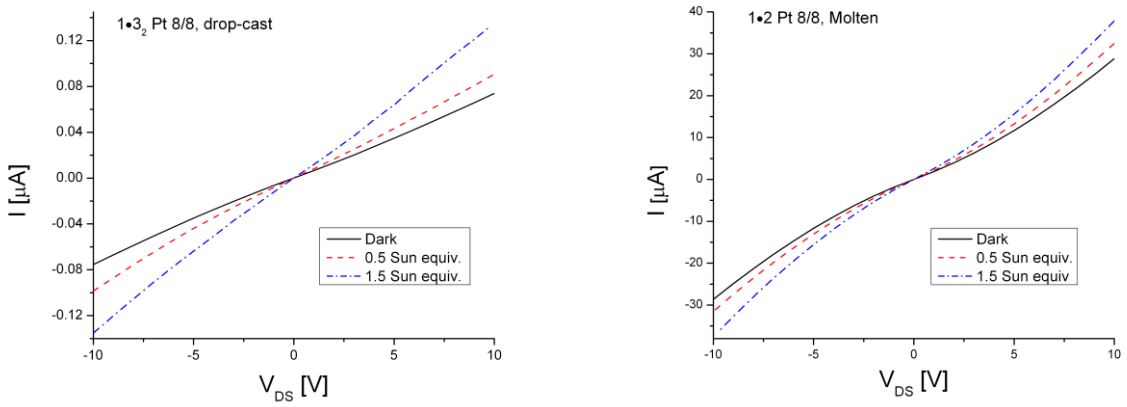

Figure 7. Effect of irradiation with white light upon the I-V characteristics of a device made from (a) **1·3**$_2$ and (b) **1·2** with 8µm channel length.

The photoconductive effect of devices made with melt-deposited (Figure 7b) and pseudo drop-cast **1·2** showed a comparable increase in resistivity (1.3 and 1.5-1.7, respectively). While a deviation from ideal Ohmic behaviour was again observed for the dark measurement, the most striking feature was the two orders of magnitude current increase for the melt-deposited sample, which is in agreement with the near total coverage and the improved electrode contacts.

Although the relative increase in conductivity was small, this was attributed to the comparatively large dark currents arising from these low bandgap semiconductors. For both compounds, the absolute conductivity showed considerable increase upon irradiation, which is congruent with the donor-acceptor system's ability to efficiently separate the generated charges. Previously-reported photoconductivity measurements of a range of single-component molecular materials, using a similar interdigitated-electrode technique [24], showed absolute values of δI

upon illumination orders of magnitude lower than we observe. This suggests that for charge-transfer complexes, the On/Off ratio may be greatly improved by lowering the dark current through reducing film thickness to lower the 'bulk' conductivity or by reducing the temperature. With optimisation of these features, charge-transfer salts may prove an attractive prospect for further photoconductivity studies.

3. Experimental

General. Compounds **1** and **6** were used as received from Aldrich. Compound **2** was prepared as described in this work and compound **3** by the known method [8]. All compounds were additionally purified by sublimation under vacuum. In the CT complex preparations, common Schlenk and glove-box techniques were used. Solvents were dried under argon with MBraun SPS-800 device.

Spectral Measurements. UV-vis spectra were obtained with a Shimadzu UV-2401PC spectrophotometer. EPR measurements were carried out with a Bruker ESP-300 spectrometer (MW power 265 mW, modulation frequency 100 kHz, and modulation amplitude 0.005 mT).

Single-crystal X-ray diffraction. The XRD data (Table 2) for complexes **1·2** and **1·3**$_2$ were collected on a Siemens P4 diffractometer using Mo Kα (λ = 0.71073 Å) radiation with a graphite monochromator. In the case of **1·2**, absorption corrections were not applied, and were made by *REFDELF* method in the case of **1·3**$_2$. With the *Olex2* program [25], the structures were solved by direct methods using the *SHELXS-97* program [26] and refined by the least-squares method in the full-matrix anisotropic (isotropic for H atoms) approximation using the *SHELXL-97* program [26]. The final structures were analyzed for exposed shortened contacts between non-bonded atoms with *PLATON* [27] and *MERCURY* [28] programs.

CCDC-?????? (for **1·2**) and ?????? (for **1·3**$_2$) contain supplementary crystallographic data for this paper. These data can be obtained free of charge from The Cambridge Crystallographic Data Centre.

Table 2. Crystal data and structure refinement for the complexes.

Compound	**1·2**	**1·3**$_2$
Empirical formula	$C_8H_4N_4S_6$	$C_{14}H_4N_8S_4Te_2$
Formula weight	348.51	667.69

Temperature [K]	173(2)	173(2)
Wavelength [Å]	0.71073	0.71073
Crystal system	Triclinic	Monoclinic
Space group	*P–1*	$P2_1/n$
Unit cell dimensions *a* [Å]	6.4030(10)	8.0879(8)
b [Å]	7.3320(10)	7.7443(15)
c [Å]	7.5660(10)	16.7567(14)
α [°]	99.090(10)	90.00
β [°]	90.280(10)	101.502(7)
γ [°]	115.380(10)	90.00
Volume [Å ^{3}]	315.84(8)	1028.5(2)
Z	1	2
Density (calcd.) [$Mg \cdot m^{-3}$]	1.832	2.156
Abs. coefficient [mm^{-1}]	1.065	3.261
F(000)	176.0	624.0
Crystal size [mm^3]	0.5 × 0.45 × 0.35	1.0 × 0.50 × 0.30
2Θ range for data collection	5.48-54.98°	5.24-54.96°
Index ranges	$-7 \le h \le 7, -9 \le k \le 9, -9 \le l \le 9$	$-10 \le h \le 1, -1 \le k \le 10, -21 \le l \le 21$
Reflections collected	2905	3313
Independent reflections	1429 [R(int) = 0.0404]	2354 [R(int) = 0.0382]
Completeness to Θ^o [%]	98.1	100.0
Data / restraints / parameters	1429 / 0 / 84	2354 / 0 / 127
Goodness-of-fit on F^2	1.130	1.182
Final R indices [$I > 2\sigma(I)$]	$R_1 = 0.0236$, $wR_2 = 0.0625$	$R_1 = 0.0255$, $wR_2 = 0.0695$
Final R indices (all data)	$R_1 = 0.0244$, $wR_2 = 0.0631$	$R_1 = 0.0264$, $wR_2 = 0.0701$
Largest diff. peak / hole / e $Å^{-3}$	0.36 / -0.28	0.87 / -1.02

Powder X-ray diffraction. Powder diffraction data for polycrystalline samples of complexes **1·2** and **1·3**$_2$ were obtained at ambient temperature with a Shimadzu XRD 7000S instrument. The samples were ground under heptane prior to measurement. Modeling the diffraction patterns from the single-crystal structures was performed with *MERCURY* [28] and *PowderCell* [29] programs (Supporting Information, Figure S2).

Thermal analysis. Thermal analysis in the range 30-500^{o}C was performed in helium atmosphere with a Hetzsch 409 PC/PG instrument equipped with a platinum pan; heat rate was 10^{o}C/min.

Electrical Conductivity Measurements. The standard two-contact method was used. Single crystals of complexes **1·2** and **1·3**$_2$ were glued to thin platinum wires by graphite conducting paste. The resistances were measured with an E-6-3 teraohmmeter.

Photoconductivity Measurements. Devices were composed of gold or platinum electrodes (200nm) on a titanium adhesion layer (5nm) deposited on a borosilicate glass wafer via photolithography and liftoff technique. The interdigitated electrode area was 2x2mm while the actual electrode width and channel length used were either 8/8 or 20/20, resulting in different length-to-width ratios of 3.1 x 10^4 and 5 x 10^3. After washing with acetone, isopropanol and chloroform, the current-voltage characteristics of these chips were then measured over a range of -10 to 10 V using a Keithley Instruments 2612A Dual-Channel System SourceMeter Instrument, first in the dark and then under illumination equivalent to 0.5 and 1.5 suns using a Sciencetech solar simulator with AM1.5 filter, calibrated with a standard Si solar cell. All measurements were carried out at room temperature and the substrate was kept under a flow of nitrogen, to minimize both the exposure to atmospheric oxygen and any potential heating of the substrate. The lack of significant heating effects was confirmed by measuring a device under continuous irradiation over a longer period of time. Compound **1·3**$_2$ was deposited by pseudo drop-casting a suspension in hexane, yielding partial coverage of the electrode surface with small crystals that were sufficiently large to bridge multiple electrode fingers. **1·2** on the other hand was deposited either via placing a number of larger flakes on the electrode surface and adding some solvent, or by subsequent heating to 100°C for 30 seconds, melting the material to the chip.

Quantum Chemical Calculations. All calculations were performed with the *GAUSSIAN09* suit of programs [30]. The B3LYP functional [31] was used since it was successfully employed earlier for calculating EA [10], as well as of properties of various closed- and open-shell chalcogen-nitrogen rings and cages including π-RAs [6,7,32]. The B97-D [15] functional was also employed in the calculations of the CT complex formation. The Def2-SVPD with diffuse basis functions and ECP was used for Te [33]. The UV-Vis spectra were calculated by time-dependent DFT [18] with B3LYP [31] and M06-HF [17] functionals. Calculations for the THF and MeCN solutions were carried out with the polarizable continuum model (IEFPCM) [34] with radii and non-electrostatic terms of the SMD solvation model [35] as implemented into

the *GAUSSIAN09* suit of programs [30]. The QTAIM calculations were performed with the *AIMAll* program [36]. The *Chemcraft* program [37] was used for visualization of the calculated molecular structures and MOs.

Preparations. Compound 2. At -5°C and under argon, 4.8 ml (0.06 mol) of S_2Cl_2 was added dropwise to a stirred solution of 2.0 g (0.02 mol) of **6** and 6.4 ml (0.08 mol) of pyridine in 200 ml of MeCN. The reaction mixture was stirred at ambient temperature for 20 h, refluxed for 7 h, cooled to 20°C, and filtered. The solvent was distilled off under reduced pressure. The residue was dissolved in 50 ml of dichloromethane, and the solution was washed with 2 x 30 ml of water and dried over $MgSO_4$. The solvent was distilled off, and the residue was sublimed under vacuum. Compound **2** was obtained in the form of long colorless needles (2.15 g, 75 %), m. p. 117-118°C (*cf.* [7]).

Complexes 1·2 and **1·3**. A mixture of 0.102 g (0.5 mmol) of compound **1** with 0.072 g (0.5 mmol) of compound **2** or 0.116 g (0.5 mmol) of compound **3** was dissolved in 15 mL of THF and solution obtained was layered with 15 mL of pentane. The system was left at -50^{o}C in the case of complex **1·2**, and at ambient temperature in the case of complex **1·3**, until solvent diffusion ceased. Solvents were removed and complex **1·2** was obtained in the form of black-green prisms (0.091 g, 54 %), and complex **1·3**$_2$ in the form of big black prisms (0.138 g, 83 %). In both cases, the crystals obtained were suitable to XRD.

Found (calculated): **1·2**: C 27.57 (27.57), H 1.28 (1.16), N 15.98 (16.07), S 55.43 (55.20); **1·3**$_2$: C 25.08 (25.18), H 0.82 (0.61), N 16.80 (16.78), S 19.32 (19.21).

Under argon, a mixture of 0.102 g (0.5 mmol) of **1** with 0.072 g (0.5 mmol) of **2** was grind in agate mortar to give dark-green powder. The powder was sublimed at static conditions 90°C / 0.1 mm in subliming unit or in sealed glass tube. Complex **1·2** was quantitatively obtained in the form of lustrous black crystals. The crystals from the sealed tube (Supporting Information, Figure S1) were suitable to XRD, whereas those from the subliming unit were not.

4. Conclusions

New CT complexes of tetrathiafulvalene (**1**) with [1,2,5]thiadiazolo[3,4-c][1,2,5]thiadiazole (**2**) and 3,4-dicyano-1,2,5-telluradiazole (**3**) were prepared in the form of single crystals to be the first complexes between **1** and 1,2,5-chalcogenadiazole derivatives. The structure of the complexes was established by X-ray diffraction as **1·2** and **1·3**$_2$, respectively.

According to the DFT calculations and UV-vis spectral measurements the complexes are weakly bonded, the CT from **1** onto **2** is 0.24e and from **1** onto two molecules of **3** 0.39e. The single crystals of the complexes revealed semiconductor properties.

Further experiments involving stronger donors, such as tetrathiatetracene [38] (0/+1 electrochemical potential: 0.15 V [39]), and acceptors, such as bis([1,2,5]thiadiazolo)[3,4-b;3',4'-e]pyrazine (-1/0 electrochemical potential: 0.10 V) [3], are in progress.

Acknowledgments

The authors are grateful to Dr. Nadezhda V. Vasilieva for cyclic voltammetry experiments on compound **3**. The authors are also grateful to the Royal Society (RS International Joint Project 2010/R3), Deutsche Forschungsgemeinschaft (project 436 RUS 113/967/0-1 R), the Russian Foundation for Basic Research (project 10-03-00735), the Presidium of the Russian Academy of Sciences (projects 7.17 and 8.14), and to the Siberian Branch of the Russian Academy of Sciences (project 105) for funding, and to the Siberian Supercomputer Center for computational facilities. N. A. S. thanks the Russian Science Support Foundation for a 2010-2011 Postgraduate Scholarship. G.T.S./N.R. thank the University of Edinburgh and the EPSRC for support.

References and Notes

1. IUPAC name: 2,2'-bis(1,3-dithiolydene).

2. All electrochemical potentials are given for MeCN solutions and vs. SCE.

3. R.T. Boere, T.L. Roemmele, *Coord. Chem. Rev.*, **2000**, *210*, 369-445.

4. a) D.L. Lichtenberger, R.L. Johnston, K. Hinkelmann, T. Suzuki, F. Wudl, *J. Am. Chem. Soc.*, **1990**, *112*, 3302-3307. b) R. Gleiter, E. Schmidt, D.O. Cowan, J.P. Ferraris, *J. Electron Spectrosc. Relat. Phenom.*, **1973**, *2*, 207-210.

5. Relative literature is too abundant to be cited completely, selected references: a) G. Saito, Y. Yoshida, *Bull. Chem. Soc. Japan*, **2007**, *80*, 1-137. b) P. Frere, P.J. Skabara, *Chem. Soc. Rev*., **2005**, *34*, 69-98. c) *Organic Conductors, Superconductor, and Magnets: From Synthesis to Molecular Electronics*, L. Ouahab, E. Yagubskii, Eds., Kluwer, **2004**. d) R.P. Shibaeva, E.B. Yagubskii, *Chem. Rev.*, **2004**, *104*, 5347-5378. e) T. Enoki, A. Miyazaki, *Chem. Rev.*, **2004**, *104*,

5449-5477. f) M. Bendikov, F. Wudl, D. Perepichka, *Chem. Rev.*, **2004**, *104*, 4891-4946. g) C. Rovira, *Chem. Rev.*, **2004**, *104*, 5289-5317.

6. a) A.V. Zibarev, R. Mews, *Selenium and Tellurium Chemistry: From Small Molecules to Biomolecules and Materials*, Eds. J.D. Woollins, R.S. Laitinen, Springer, **2011**, pp. 123-149. b) N.P. Gritsan, A.V. Zibarev, *Izv. AN. Ser. Khim.*, **2011**, *60*, 2091-2100 (in Russian).

7. A.Yu. Makarov, I.G. Irtegova, N.V. Vasilieva, I.Yu. Bagryanskaya, T. Borrmann, Yu.V. Gatilov, E. Lork, R. Mews, W.-D. Stohrer, A.V. Zibarev, *Inorg. Chem.* **2005**, *44*, 7194-7199.

8. a) N.A. Semenov, N.A. Pushkarevsky, J. Beckmann, P. Finke, E. Lork, R. Mews, I.Yu. Bagryanskaya, Yu.V. Gatilov, S.N. Konchenko, V.G. Vasiliev, A.V. Zibarev, *Eur. J. Inorg. Chem.* **2012** (doi: 10.1002/ejic.201200376). b) A.F. Cozzolino, Q. Yang, I. Vargas-Baca, *Cryst. Growth Des.* **2010**, *10*, 4959-4964.

9. a) E.A. Suturina, N.A. Semenov, A.V. Lonchakov, I.Yu. Bagryanskaya, Yu.V. Gatilov, I.G. Irtegova, N.V. Vasilieva, E. Lork, R. Mews, N.P. Gritsan, A.V. Zibarev, *J. Phys. Chem. A* **2011**, *115*, 4851-4860. b) V. Bertini, F. Lucchesini, A. De Munno, *Synthesis* **1982**, *8*, 681-683.

10. J.C. Rienstra-Kiracofe, G.S. Tschumper, H.F. Schaefer, S. Nandi, G.B. Ellison, *Chem. Rev.*, **2002**, *102*, 231-282.

11. B. Milian, R. Pou-Amerigo, R. Viruela, E. Orti, *Chem. Phys. Lett.*, **2004**, *391*, 148-151.

12. a) P. Kebarle, S. Chowdhury, *Chem. Rev.*, **1987**, *87*, 513-543. b) M.L. Kaplan, R.C. Haddon, F.B. Bramwell, F. Wudl, J.H. Marshall, D.O. Cowan, S. Gronowitz, *J. Chem. Phys.*, **1980**, *84*, 427-431.

13. a) *Heterocyclic Compounds*, Ed. R.C. Elderfield, Wiley, **1950**, Vol. 1. b) Q. Li, Y. Xu, C. Liu, J. Kim, *Catal. Lett.* **2008**, *122*, 354-358. c) A.V. Mashkina, *Chem. Heterocycl. Comp.* **2010**, 46, 1063-1067.

14. W.F. Cooper, N.C. Kenny, J.W. Edmonts, A. Nagel, F. Wudl, P. Coppens, *Chem. Commun.*, **1971**, 889-890.

15. S.J. Grimme, *Comput. Chem*., **2006**, *27*, 1787–1799.

16. a) *The Quantum Theory of Atoms in Molecules*; Eds. C.F. Motta, R.J. Boid, Wiley, **2007**. b) R.F.W. Bader, *Monat. Chem.*, **2005**, *136*, 819-856. c) R.F.W. Bader, *Atoms in Molecules: A Quantum Theory*; Oxford University Press, **1990**.

17. a) Y. Zhao, D.G. Truhlar, *Acc. Chem. Res*., **2008**, *41*, 157-167. b) Y. Zhao, D.G. Truhlar, *J. Phys. Chem. A*, **2006**, *110*, 13126-13130.

18. A. Dreuw, M. Head-Gordon, *Chem. Rev.*, **2005**, *105*, 4009-4037.

19. B. Paiz, S. Suhai, *J. Compt. Chem.*, **1998**, *18*, 575-584.

20. Secondary bonding interactions (supramolecular synthons) N…X (X = S, Se, Te) are relatively strong for X = Te and very weak for X = S: a) A.F. Cozzolino, P.J.W. Elder, I. Vargas-Baca, *Coord. Chem. Rev.* **2011**, *255*, 1426-1438. b) A.F. Cozzolino, I. Vargas-Baca, S. Mansour, A.H. Mahmoudkhani, *J. Am. Chem. Soc.*, **2005**, *127*, 3184-3190.

21. A.J. Zhou, S.L. Zheng, Y. Fang, M.L. Tong, *Inorg. Chem.*, **2005**, *44*, 4457-4459.

22. M. Chollet, L. Guerin, N. Uchida, S. Fukaya, H. Shimoda, T. Ishikawa, K. Matsuda, T. Hasegawa, A. Ota, H. Yamochi, G. Saito, R. Tazaki, S. Adachi, S. Koshihara, *Science*, **2005**, *307*, 86-89

23. M. M. Matsushita, H. Kawakami, E. Okabe, H. Kouka, Y. Kawada, T. Sugawara, *Polyhedron*, **2005**, *24*, 2870-2875

24. N. V. Tkachenko, V. Chukharev, P. Kaplas, A. Tolkki, A. Efimov, K. Haring, J. Viheriala, T. Niemi, H. Lemmetyinen, *Applied Surface Science* **2010**, *256*, 3900–3905

25. O.V. Dolomanov, L.J. Bourhis, R.J. Gildea, J.A.K. Howard, H. Puschmann, *J. Appl. Cryst.* **2009**, *42*, 339-341.

26. G.M. Sheldrick, *Acta Crystallogr. A*, **2008**, *64*, 112-122.

27. a) A.L. Spek, *PLATON, A Multipurpose Crystallographic Tool, Version 10M*, Utrecht University, The Netherlands, **2003**. b) A.L. Spek, *J. Appl. Crystallogr.*, **2003**, *36*, 7-13.

28. C.F. Macrae, P.R. Edgington, P. McCabe, E. Pidcock, G.P. Shields, R. Taylor, M. Towler, J. van de Stree, *J. Appl. Crystallogr.*, **2006**, *39*, 453-457.

29. W. Kraus, G. Nolze, *PowderCell 2.3* (ccp14.ac.uk/tutorial/powdcell).

30. M.J. Frisch, G.W. Trucks, H.B. Schlegel, G.E. Scuseria, M.A. Robb, J.R. Cheeseman, G. Scalmani, V. Barone, B. Mennucci, G.A. Petersson, H. Nakatsuji, M. Caricato, X. Li, H.P. Hratchian, A.F. Izmaylov, J. Bloino, G. Zheng, J.L. Sonnenberg, M. Hada, M. Ehara, K. Toyota, R. Fukuda, J. Hasegawa, M. Ishida, T. Nakajima, Y. Honda, O. Kitao, H. Nakai, T. Vreven, J.A. Montgomery, J.E. Peralta, F. Ogliaro, M. Bearpark, J.J. Heyd, E. Brothers, K.N. Kudin, V.N. Staroverov, R. Kobayashi, J. Normand, K. Raghavachari, A. Rendell, J.C. Burant, S.S. Iyengar,

J. Tomasi, M. Cossi, N. Rega, N.J. Millam, M. Klene, J.E. Knox, J.B. Cross, V. Bakken, C. Adamo, J. Jaramillo, R. Gomperts, R.E. Stratmann, O. Yazyev, A.J. Austin, R. Cammi, C. Pomelli, J.W. Ochterski, R.L. Martin, K. Morokuma, V. G. Zakrzewski, G.A. Voth, P. Salvador, J.J. Dannenberg, S. Dapprich, A.D. Daniels, Ö. Farkas, J.B. Foresman, J.V. Ortiz, J. Cioslowski, D.J. Fox, *Gaussian 03, Revision E.01*, Gaussian, Inc., Wallingford CT, **2004**.

31. a) A.D. Becke, *J. Chem. Phys.*, **1993**, *98*, 5648-5652. b) C. Lee, W. Yang, R.G. Parr, *Phys. Rev. B*, **1988**, *37*, 785-789.

32. a) S.N. Konchenko, N.P. Gritsan, A.V. Lonchakov, U. Radius, A.V. Zibarev, *Mendeleev Commun.*, **2009**, *19*, 7-9. b) N.A. Semenov, N.A. Pushkarevsky, A.V. Lonchakov, A.S. Bogomyakov, E.A. Pritchina, E.A. Suturina, N.P. Gritsan, S.N. Konchenko, R. Mews, V.I. Ovcharenko, A.V. Zibarev, *Inorg. Chem.*, **2010**, *49*, 7558-7564. c) S.N. Konchenko, N.P. Gritsan, A.V. Lonchakov, I.G. Irtegova, R. Mews, V.I. Ovcharenko, U. Radius, A.V. Zibarev, *Eur. J. Inorg. Chem.*, **2008**, 3833-3838. d) N.P. Gritsan, A.V. Lonchakov, E. Lork, R. Mews, E.A. Pritchina, A.V. Zibarev, *Eur. J. Inorg. Chem.*, **2008**, 1994-1998.

33. a) D. Rappoport, F. Furche, *J. Chem. Phys*., **2010**, *133*, 134105 (article number). b) K.L. Schuchardt, B.T. Didier, T. Elsethagen, L Sun, V. Gurumoorthi, J. Chase, J. Li, T.L.J. Windus, *Chem. Inf. Model*., **2007**, *47*, 1045-1052. c) K.A. Peterson, D. Figgen, E. Goll, H. Stoll, M. Dolg, *J. Chem. Phys*., **2003**, *119*, 11113-11123. c) D. Feller, *J. Comp. Chem.*, **1996**, *17*, 1571-1586.

34. a) J. Tomasi, B. Mennucci, R. Cammi, R. *Chem. Rev.*, **2005**, *105*, 2999-3093. b) V.Barone, A. Polimeno, *Chem. Soc. Rev.*, **2007**, *36*, 1724-1731.

35. A.V. Marenich, C.J. Cramer, D.G. Truhlar, *J. Phys. Chem. B*, **2009,** *113*, 6378-6396.

36. T.A. Keith, *AIMAll, Version 10.03.25* (aim.tkgristll.com).

37. *Chemcraft Version 1.6. Build 350* (chemcraftprog.com).

38. IUPAC name: tetraceno[5,6-cd:11,12-c'd']bis[1,2]dithiole.

39. a) I.F. Schegolev, E.B. Yagubskii, *Extended Linear Chain Compounds*, Ed. J.S. Miller, Plenum Press, **1982**, Vol. 2, p. 385-416. b) E.B. Yagubskii, *Mol. Cryst. Liq. Cryst.*, **2002**, *380*, 15-21. c) S. Sekizaki, C. Tada, H. Yamochi, G. Saito, *J. Mater. Chem.*, **2001**, *11*, 2293-2302.